DOI 10.1007/s11003-021-00454-0
Materials Science, Vol. 56, No. 4, January, 2021 (Ukrainian Original Vol. 56, No. 4, July–August, 2020)

INFLUENCE OF HEAT TREATMENT ON THE MICROSTRUCTURE AND PHYSICOMECHANICAL PROPERTIES OF TITANIUM ALLOYS OF THE Ti–Nb–Mo SYSTEM

O. M. Myslyvchenko,[1,2] A. A. Bondar,[1] N. I. Tsyganenko,[1] V. M. Petyukh,[1] Yu. F. Lugovskyi,[1] and V. F. Gorban[1]

We present the results of investigation of the structure and properties of four titanium alloys of the Ti–Nb–Mo system after their subsolidus annealing and annealing with quenching from 870°C. The obtained results indicate that heat treatment strongly affects the phase composition, microstructure, microhardness, Young's modulus, and elastic properties of investigated specimens. The annealed alloys are two-phase $\alpha' + \beta$ alloys and their Young's modulus is close to Young's modulus of pure titanium (87–100 GPa). Quenching leads to the formation of the α''-phase and the amount of β-phase becomes insignificant. As a result, the microhardness somewhat decreases and Young's modulus becomes ~ 1.5 times lower.

Keywords: titanium alloys, modulus of elasticity, rhombic martensite.

Introduction

In recent years, the demand of contemporary medicine for metallic implants permanently increases. The implantation of any biomaterial is accompanied by its direct contact with tissues and media of the human organism. Thus, the materials used for implants must guarantee not only the required mechanical and chemical biocompatibility but also high wear and corrosion resistances, strength, and ability to be integrated with biological media. As one of important characteristics of medical alloys intended for the replacement of the bone tissues, we can mention the elasticity modulus, which determines the functional reliability of implants under the actual conditions of operation in human bodies. In order to guarantee the optimal redistribution of stresses and prevent the premature degradation of the bone tissue, the modulus of elasticity of the implant should be close to the modulus of elasticity of the bone (~ 40 GPa).

At present, titanium and alloys based on titanium nickelide (TiNi) are the most widespread materials used for the production of bone implants. Titanium nickelide is extensively used in the medical practice. However, it contains nickel, which exerts negative influence on the living organisms [1]. For this reason, nickel-free metallic implants of the Ti–Nb, Ti–Mo, and other systems were investigated in [2–6]. In the tensile tests carried out under the conditions of cyclic loading and unloading, alloys of the Ti–Nb system underwent the inverse martensite transformation between the rhombic α''-martensite phase and the initial phase and exhibited the property of superelasticity and low induction stress of the martensite transformation (~ 200 MPa) [7]. At the same time, alloys of the Ti–Mo system have low elasticity but high induction stress of the martensite transformation under

[1] Frantsevych Institute for Problems in Materials Science, National Academy of Sciences of Ukraine, Kyiv.
[2] Corresponding author; e-mail: zvyagina47@gmail.com.

Translated from Fizyko-Khimichna Mekhanika Materialiv, Vol. 56, No. 4, pp. 44–52, July–August, 2020. Original article submitted February 4, 2020.

the conditions of cyclic tensile loading–unloading [8]. This is why, for implants, the researchers now actively develop materials of the Ti–Nb–Mo system, which combine the required properties, namely, low Young's modulus, the absence of toxic action upon the organisms, and high levels of strength and elasticity [9–12]. Surveys of publications concerning the Ti–Nb–Mo system were presented in [13, 14]. Note that phase equilibria were investigated in the solid state [15, 16]. At the same time, the melting point and metastable phase transformations are studied insufficiently.

The aim of the present work is to study the influence of heat treatment on the phase composition, microstructure, and physicomechanical properties of titanium alloys of the Ti–Nb–Mo system, which were investigated in the cast state in [17].

Methods

As source materials, we used (wt.%): titanium iodide (99.9 Ti); high-purity molybdenum rods (99.97 Mo with impurities of 0.01 Fe, 0.002 Al, 0.002 Ni, 0.003 Si, 0.0005 Ca + Mg, 0.004 C, and 0.002 O), and NbSh-00 niobium (with impurities of 0.05 Ta, 0.02 Fe, < 0.03 N, < 0.03 C, < 0.03 O, 0.009 Ti, and 0.009 Si). Alloys used for investigations were obtained as a result of melting in an electric-arc furnace with the help of a tungsten nonconsumable electrode on the copper hearth with water cooling. Melting was performed in a protective argon atmosphere (under a pressure of 50–80 kPa). The procedure of cleaning was carried out by preliminary melting of titanium getter for 5 min. The charge was melted under the conditions of weak burning of the arc and then remelted by turning over five times. First, we obtained two samples (15 g) of each alloy, which were smelted into a dingle sample with a mass of 30 g in the last stage. The rate of cooling of the ingots was ~ 80–100°C/sec. The composition of the alloys obtained for investigation was monitored by analyzing the total mass losses in the course of smelting. Since they did not exceed 0.15 wt.%, it was assumed that the alloys have the same compositions as the compositions of the charge.

The alloys were annealed at a temperature of 1600°C for 10 h in an ShVL-0,6.2/25 furnace in an argon atmosphere gettered with titanium chips. This temperature is lower (by 80–125°C) than the initial points of melting obtained by the differential thermal analysis (DTA). The annealed samples were repeatedly heated in air for 1–2 min up to a temperature of 870°C and then quenched in water. Then the samples were ground with abrasive paper with different grit sizes and polished with a chromium-oxide suspension. In order to study the microstructure in the course of etching, we used the Kroll etching agent (8 mliter HF, 20 mliter HNO_3, and 62 mliter H_2O).

The X-ray investigations were carried out in a DRON-3 diffractometer in the CoK_α-radiation. The X-ray diffraction patterns were taken by the method of step-by-step scanning with intervals of 0.05° and holding times of 1–2 sec. The microstructure was investigated with the help of an MIM-7 optical microscope. The DTA was carried out in a device equipped with a sensor similar to the sensor developed in [18]. As a protective medium, we used high-purity helium under a pressure of 100 kPa. The samples were placed in ceramic crucibles made of Sc_2O_3.

To determine the modulus of elasticity, we used ultrasonic vibrations [19] and microindentation. It was determined as the mean value of measurements carried out for two specimens. The specimens had the shape of rods with square cross section $25 \times 2 \times 2$ mm in size. The selected length of the specimens guaranteed the resonance frequency of longitudinal vibrations equal to ~ 100 kHz. The modulus of elasticity was determined as follows: $E = 4\rho l^2 f^2$, where l is the length of the specimen, f is the frequency of natural longitudinal vibrations, and ρ is density. The density of the investigated materials was measured by hydrostatic weighing. The procedure of microindentation was carried out in a "Mikron-Gamma" device under a load of 2.94 N applied to a Berkovich diamond pyramid with an apex angle of 65°.

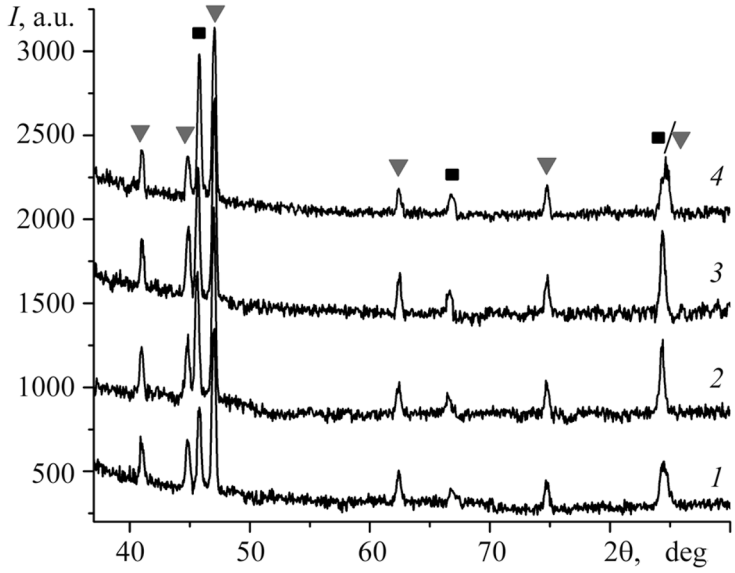

Fig. 1. X-ray diffraction patterns of alloys of the Ti–Nb–Mo system annealed at 1600°C for 10 h: (1) $Ti_{94}Nb_4Mo_2$; (2) $Ti_{95.5}Nb_{1.5}Mo_3$; (3) $Ti_{92.5}Nb_5Mo_{2.5}$; (4) $Ti_{94}Nb_2Mo_4$; (▼) α; (■) β.

Loading and unloading were performed automatically for 30 sec. We simultaneously recorded the diagrams of loading, holding, and unloading on the $F-h$ coordinates (h is the depth of penetration of the indenter). The device automatically calculates the values of hardness (H), contact modulus of elasticity (E_r), elastic strains (ε_{es}), and yield strength (σ_{es}) [20].

Results and Discussion

According to the results of X-ray diffraction (XRD) analysis, the phase compositions of four investigated alloys annealed at a subsolidus temperature are mixtures of two phases, namely, the hexagonal α-phase and the cubic β-phase (Fig. 1). It was established that in all investigated alloys, the lattice constants are close and weakly depend on the composition (Table 1). An increase in the content of alloying elements (especially of molybdenum) leads to a certain increase in the content of the β-phase with the molybdenum equivalent of the alloy, which is computed as follows: Mo_{eqv} = %Mo + (%Nb/3.3), where %Mo and %Nb are the contents of the corresponding metals in at.%.

The results of optical microscopy (Fig. 2) are in good agreement with the XRD data and show that all alloys have heterophase structures. An attempt to analyze the microstructure with the help of scanning electron microscopy did not give the desired results because we did not observe any contrast between the phase components. This means that the mean atomic numbers of the indicated two phase components (i.e., their chemical compositions) are close.

The microhardnesses of annealed alloys vary within the range 3.0–3.6 GPa (Fig. 3a). The $Ti_{94}Nb_4Mo_2$ alloy (with the lowest content of the phase based on β-titanium) has the lowest microhardness. At the same time, the $Ti_{92.5}Nb_5Mo_{2.5}$ and $Ti_{94}Nb_2Mo_4$ alloys have the highest microhardness.

Young's moduli of the annealed alloys (Fig. 4a) are close to the Young's modulus of pure titanium (87–100 GPa). Despite the fact that the molybdenum equivalent (Table 1) and, hence, the content of the β-phase in $Ti_{94}Nb_2Mo_4$ alloy take the highest values, this alloy is not characterized by a low value of Young's modulus (as compared with the the other alloys).

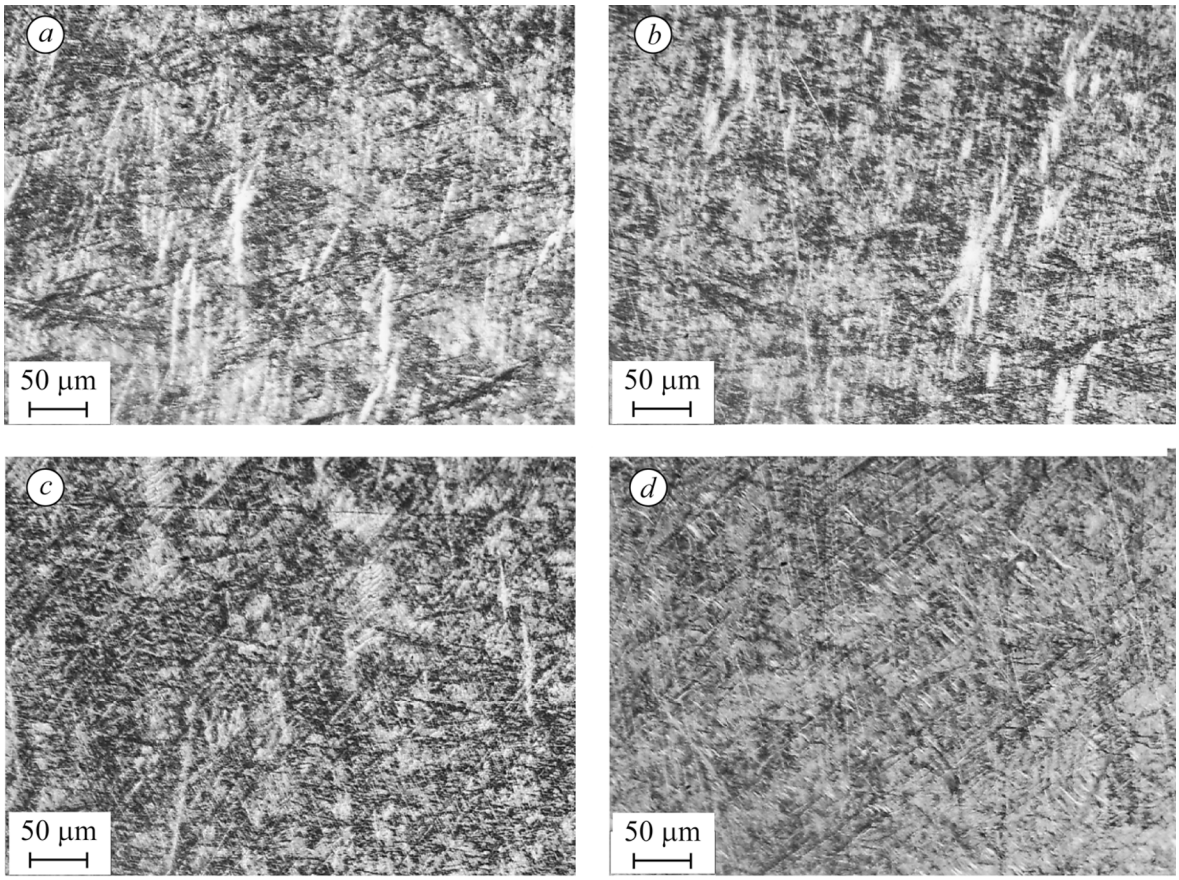

Fig. 2. Optical microscopy of alloys of the Ti–Nb–Mo system annealed at 1600°C for 10 h: (a) $Ti_{94}Nb_4Mo_2$; (b) $Ti_{95.5}Nb_{1.5}Mo_3$; (c) $Ti_{92.5}Nb_5Mo_{2.5}$; (d) $Ti_{94}Nb_2Mo_4$.

Table 1
Lattice Constants and Mass Content of Phases According to the Results of the XRD Analysis of Alloys of the Ti–Nb–Mo System Annealed at 1600°C for 10 h

Alloy	Composition (at.%)	Molybdenum equivalent	α		β	
			contents, wt.%	lattice constants, nm	contents, wt.%	lattice constants, nm
1	$Ti_{94}Nb_4Mo_2$	3.2	72	$a = 0.2946$; $c = 0.4685$	28	$a = 0.3260$
2	$Ti_{95.5}Nb_{1.5}Mo_3$	3.4	69	$a = 0.2946$; $c = 0.4686$	31	$a = 0.3260$
3	$Ti_{92.5}Nb_5Mo_{2.5}$	4.0	65	$a = 0.2946$; $c = 0.4687$	35	$a = 0.3260$
4	$Ti_{94}Nb_2Mo_4$	4.6	62.5	$a = 0.2947$; $c = 0.4687$	37.5	$a = 0.3261$

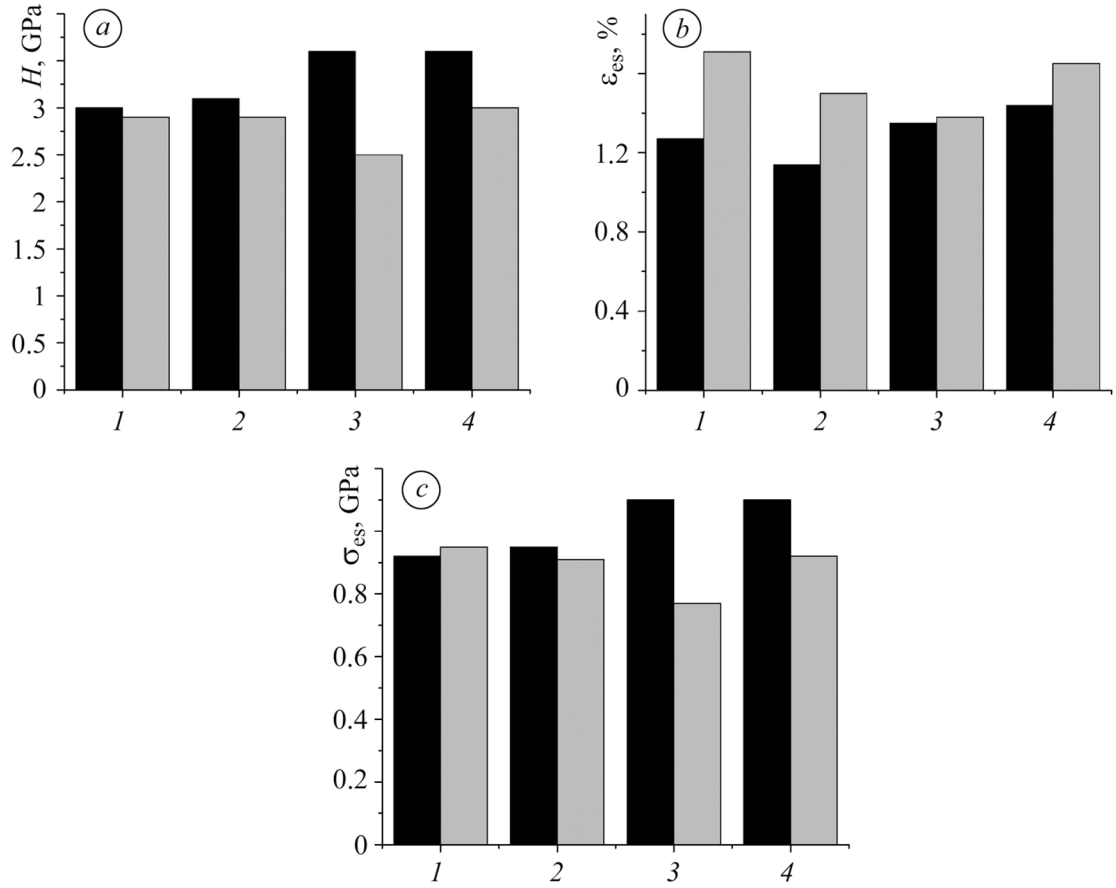

Fig. 3. Microhardness (a), elastic strains (b), and yield strength (c) of alloys of the Ti–Nb–Mo system annealed at 1600°C for 10 h (dark columns) and annealed with subsequent quenching from 870°C (gray columns): (1) $Ti_{94}Nb_4Mo_2$; (2) $Ti_{95.5}Nb_{1.5}Mo_3$; (3) $Ti_{92.5}Nb_5Mo_{2.5}$; (4) $Ti_{94}Nb_2Mo_4$.

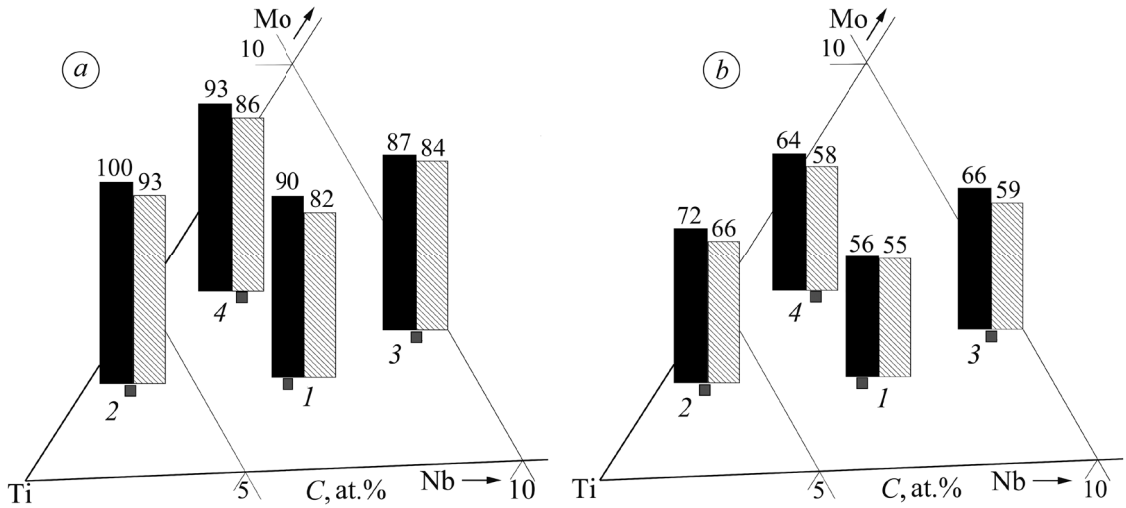

Fig. 4. Young's moduli of alloys of the Ti–Nb–Mo system annealed at 1600°C for 10 h (a) and alloys annealed at 1600°C for 10 h with subsequent quenching from 870°C (b): (1) $Ti_{94}Nb_4Mo_2$; (2) $Ti_{95.5}Nb_{1.5}Mo_3$; (3) $Ti_{92.5}Nb_5Mo_{2.5}$; (4) $Ti_{94}Nb_2Mo_4$; (▩) composition of the alloys; (■) and (▨) Young's moduli (GPa) obtained according to the results of the methods of ultrasonic oscillations and microindentation, respectively.

Table 2
Temperatures of Phase Transformations (°C) in Alloys of the Ti–Nb–Mo System Annealed at 1600°C for 10 h According to the Results of DTA

Alloy	Composition, at.%	Heating				Cooling	
		Onset of the $\alpha' \rightarrow \beta$-transformation	End of the $\alpha' \rightarrow \beta$-transformation	Onset of melting	End of melting	Onset of crystallization	Onset of the $\beta \rightarrow \alpha'$-transformation
1	$Ti_{94}Nb_4Mo_2$	570	794	1726	1765	1777	774
2	$Ti_{95.5}Nb_{1.5}Mo_3$	522	816	1683	1750	1758	798
3	$Ti_{92.5}Nb_5Mo_{2.5}$	560	771	1725	1773	1774	716
4	$Ti_{94}Nb_2Mo_4$	682	796	1718	1763	1768	743

As follows from the accumulated results (Fig. 4a), the elasticity moduli determined by the method of indentation take lower values, which is possibly connected both with the accuracy of measurements (indentation is an indirect method of measuring the elasticity modulus) and with the changes in the fine structure of the specimen (because the indentation of the indenter into the specimen is accompanied by its deformation on a level of 8–10%). At the same time, the acoustic method does not involve deformation and, therefore, does not change the density of dislocations.

The investigated annealed alloys have much lower characteristics of elastic strains under the conditions of indentation than the corresponding characteristics for quenched alloys (Fig. 3b). The maximum elastic strain is observed in alloy No. 4 (1.44%). Unlike this parameter, the yield strength correlates with microhardness (Fig. 3c), namely, its lowest value is observed for alloy No. 1 (0.92 GPa) and the highest value is detected in alloys No. 3 and No. 4 (1.1 GPa). The dependences of the level of elastic strains and yield strength on the contents of phase components can hardly be detected.

The temperatures of the phase transformations were determined with the help of DTA of the specimens annealed at 1600°C for 10 h and homogenized (Table 2 and Fig. 5). In the DTA curves of all alloys, we can distinguish two sections: the thermal effect of the low-energy $\alpha \rightarrow \beta$-transformation (extended peak in the curve of heating at 522–682°C) corresponding to the extended peak of the $\beta \rightarrow \alpha$-transformation (a section in the curves of cooling within the temperature range 771–816°C) and the peaks corresponding to melting (in the course of heating) and crystallization (in the course of cooling). It is worth noting that the $(\alpha \rightarrow \beta)$-polymorphic transformation in the course of heating occurs at a temperature much lower than the temperature of the $\alpha \rightarrow \beta$-transformation in pure titanium (882°C).

As could be expected, the alloy with the minimal titanium content has the highest melting point, whereas the alloy with the maximal titanium content has the lowest melting point. For quenching, by using the DTA results on the temperature ranges of the $\alpha \rightarrow \beta$-transformation (Table 2), we choose a temperature of 870°C, which is higher than the highest temperature of existence of the α-phase.

The X-ray diffraction patterns of alloys preliminarily annealed at 1600°C for 10 h and quenched from 870°C are presented in Fig. 6. Their analysis shows that, during the heat treatment, the hexagonal martensite α-phase transforms into the rhombic α''-phase. The α- and α''-phases are similar and can hardly be distinguished by the X-ray phase diffraction analysis. However, the diffraction maximum (020) at an angle $2\theta = 42.1°$

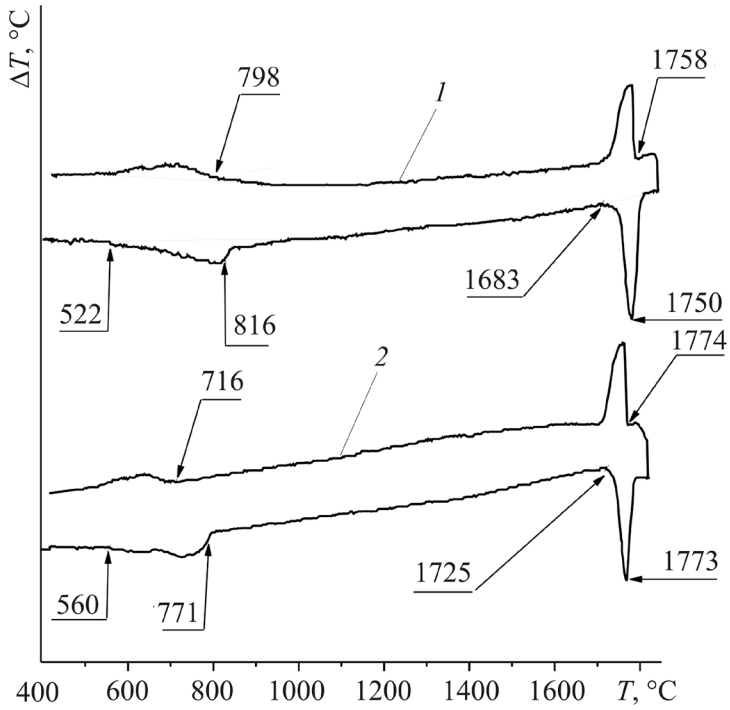

Fig. 5. DTA curves for alloys No. 2 (1) and No. 3 (2) after annealing at 1600°C for 10 h taken at a rate of 20°C/min (the curves are shifted in the vertical direction).

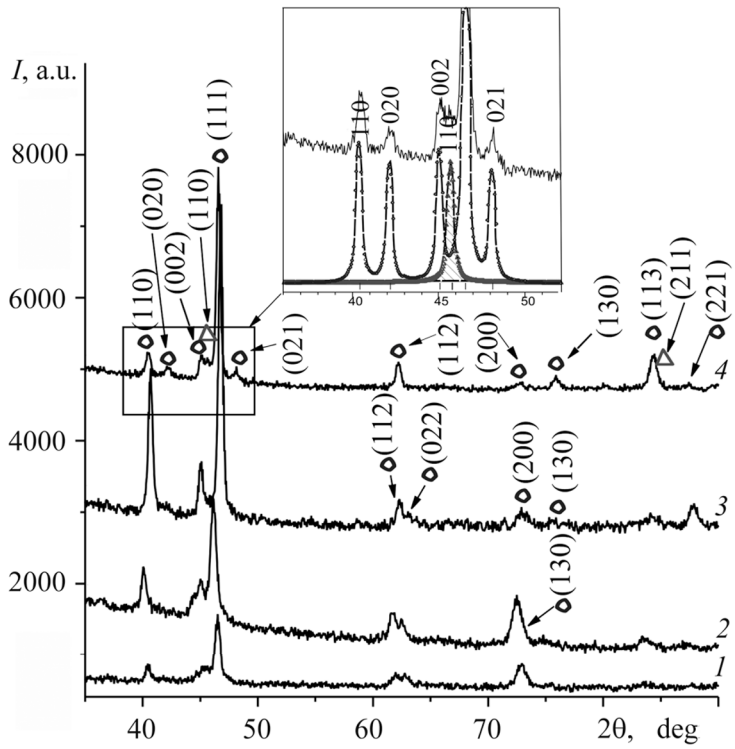

Fig. 6. X-ray diffraction patterns of alloys of the Ti–Nb–Mo system annealed at 1600°C for 10 h and then quenched from 870°C: (1) $Ti_{94}Nb_4Mo_2$; (2) $Ti_{95.5}Nb_{1.5}Mo_3$; (3) $Ti_{92.5}Nb_5Mo_{2.5}$; (4) $Ti_{94}Nb_2Mo_4$; (△) β; (○) α″.

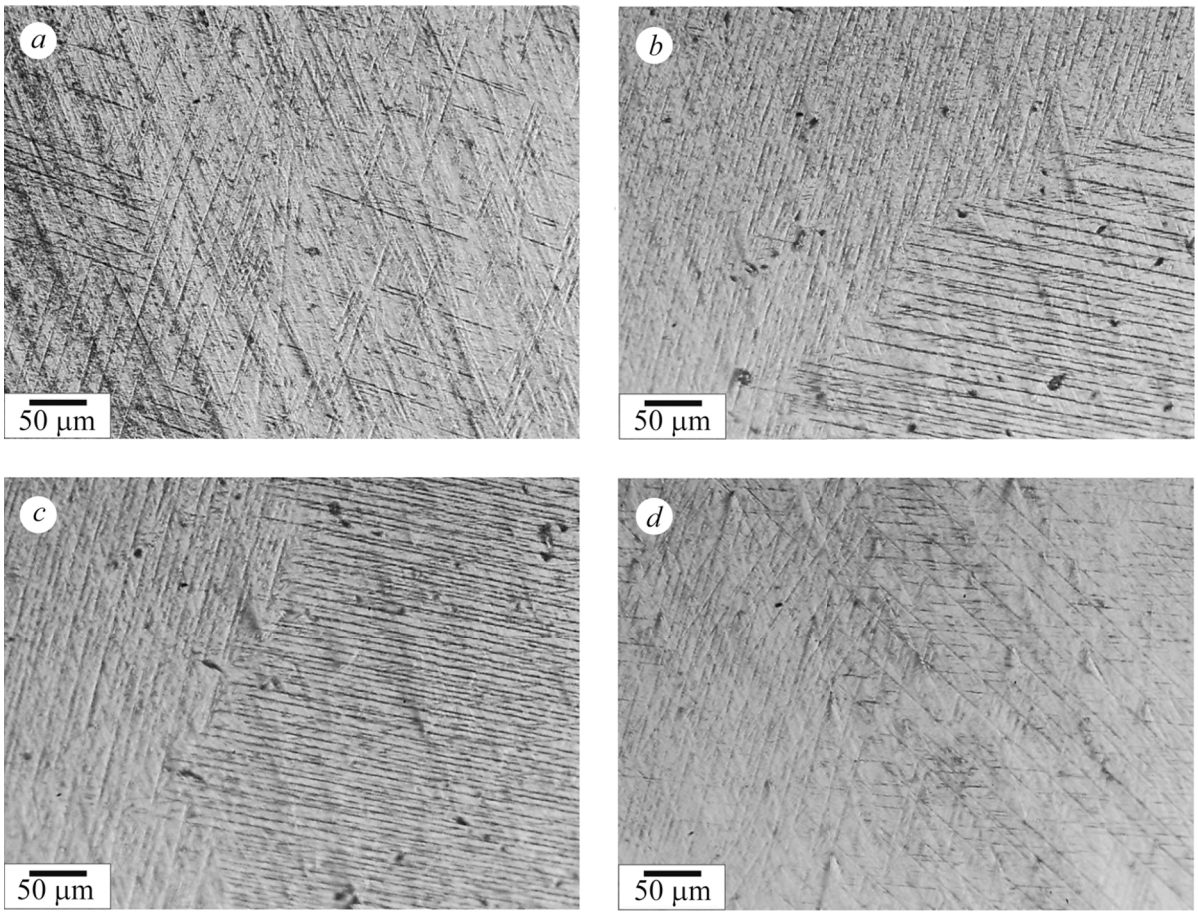

Fig. 7. Optical microscopy of alloys of the Ti–Nb–Mo system annealed at 1600°C for 10 h and then quenched from 870°C: (a) $Ti_{94}Nb_4Mo_2$; (b) $Ti_{95.5}Nb_{1.5}Mo_3$; (c) $Ti_{92.5}Nb_5Mo_{2.5}$; (d) $Ti_{94}Nb_2Mo_4$.

and the separated peaks (112) (022) and (200) (130) at angles of 62.5 and 72.0°, respectively, serve as direct indications of existence of the rhombic α″-phase whose crystal lattice is more distorted and has a lower symmetry as compared with the hexagonal α-phase. At first sight, it seems that quenched specimens have a single phase. However, a more careful analysis of all X-ray diffraction patterns reveals small amounts of the β-phase: two diffraction maxima (110) and (211) at angles $2\theta = 45.9°$ and 84.9°, respectively (see the inset in Fig. 6). In the quenched state, these alloys are characterized by crystallographic textures and high internal stresses, which lead to broadening of the diffraction maxima and decrease their intensity. All these arguments make it difficult to correctly determine the contents of the phase components.

The microstructures of quenched alloys in reflected light beams are shown in Fig. 7. In all alloys, we observe the acicular martensite α″-phase in the form of parallel strips and, most likely, with identical orientation inside each grain. Acicular precipitates of the α″ -phase are uniformly distributed over the entire area of each specimen. At the same time, in [21], these precipitates were mainly concentrated on the grain boundaries in $Ti_{72.5}Nb_{26}Si_{1.5}$ alloy.

Significant influence of heat treatment on the phase composition and microstructure of the investigated alloys is accompanied by changes in their physicomechanical properties. Thus, the α″-phase in quenched alloys has a lower hardness than the α/α′-phase in the annealed alloys (see Fig. 3a). The stresses in the α/α′- and α″-phases of the Ti–Mo system were computed in [22]. It was shown that, in the α″-phase, they are lower.

This is explained by the fact that the α''-phase can be formally regarded as an intermediate phase in the $\beta \rightarrow \alpha$-transformation. In the case where the shift of atoms is incomplete, we observe the formation of the rhombic α''-phase. At the same time, if the shift is complete, then we get the α/α'-phases. The incomplete shift in the process of formation of the α''-phase requires much smaller displacements than in the case of formation of the α/α'-phases in the course of rapid cooling. The shifts of atoms by small distances result in a smaller hardening as a result of the formation of lower stresses in the crystal lattice. This explains the fact that the hardness of alloys with predominant contents of the α''-phase is lower than the hardness of alloys in which the α/α'-phases are predominant [22].

The formation of the metastable α''-phase in the course of quenching leads to the improvement of the elastic properties of all alloys. It should be emphasized that the most pronounced increase occurs in alloy No. 1 with the lowest molybdenum equivalent. The dependence of the yield strength on the composition of alloys (see Fig. 3c) is similar to the dependence of microhardness of quenched specimens (Fig. 3a). Note that the lowest value of yield strength was detected for alloy No. 3. However, the influence of quenching on Young's modulus is especially pronounced (see Fig. 4b). Indeed, the elasticity moduli of quenched alloys become ~ 1.5 times lower as compared with the elasticity moduli of annealed alloys (Fig. 4a). According to the literature data, the α''-phase has the lowest Young's modulus in the Ti–Mo system [4]. It is formed at high cooling rates and its content increases with the molybdenum equivalent of alloying admixtures (Mo_{eq}). Here, we can also mention another result: the alloy with the minimum Mo_{eq} has the lowest Young's modulus (No. 1).

Assume that the amount of the β-phase in quenched alloys of the Ti–Nb–Mo system also increases with Mo_{eq} and that the presence of this phase causes an increase in Young's modulus. However, this observation does not explain why alloy No. 2 has the highest elasticity modulus among all investigated materials in the quenched state. Most likely, this is the result of precipitation of the other phases that are not detected in the X-ray diffraction patterns and are not visible in the optical microphotographs. This is why, for our subsequent investigations, we propose to use transmission electron microscopy.

CONCLUSIONS

In the annealed alloys, in the process of heating and cooling by the DTA method, we discovered the α'/β polymorphic transformation and the effects of melting/crystallization. In the course of quenching of the annealed alloys, we observe the transformation of the α'-martensite phase into the α''-phase, and the β-phase is partially preserved. The microstructures of quenched alloys contain colonies of acicular α''-martensite. The microhardness of the annealed alloys increases with the content of the β-phase, which correlates with the molybdenum equivalent of alloying admixtures. Quenching leads to the decrease in hardness and the improvement of the elastic properties. The annealed alloys have elasticity moduli close to the elasticity modulus of pure titanium, whereas quenching makes it possible to make this parameter about ~ 1.5 times smaller.

The present work was performed within the framework of the program of scientific investigations at the Department of Physicotechnical Problems of Materials Science of the National Academy of Sciences of Ukraine; Topic III-10-19 (state registration number 0119U100778).

REFERENCES

1. T. Rae, "The toxicity of metals used in orthopedic prostheses. An experimental study using cultured human synovial fibroblasts," *J. Bone Joint Surg. Br.*, **63**, No. 3, 435–440 (1981).

2. F. Sun, Y. L. Hao, S. Nowak, T. Gloriant, P. Laheurte, and F. Prima, "A thermo-mechanical treatment to improve the superelastic performances of biomedical Ti–26Nb and Ti–20Nb–6Zr (at.%) alloys," *J. Mech. Behav. Biomed. Mater.,* **4**, No. 8, 1864–1872 (2011).
3. Y. W. Chaia, H. Y. Kima, H. Hosodab, and S. Miyazaki, "Interfacial defects in Ti–Nb shape memory alloys," *Acta Mater.,* **56**, No. 13, 3088–3097 (2008).
4. W. F. Ho, C. P. Ju, and J. H. C. Lin, "Structure and properties of cast binary Ti–Mo alloys," *Biomaterials,* **20**, No. 22, 2115–2122 (1999).
5. D. J. Lin, C. C. Chuang, J. H. Chern, J. W. Lee, C. P. Ju, and H. S. Yin, "Bone formation at the surface of low modulus Ti–7.5 Mo implants in rabbit femur," *Biomaterials,* **28**, No. 16, 2582–2589 (2007).
6. N. T. C. Oliveira and A. C. Guastaldi, "Electrochemical stability and corrosion resistance of Ti–Mo alloys for biomedical applications," *Acta Biomater.,* **5**, No. 1, 399–405 (2009).
7. H. Y. Kim, S. Hashimoto, J. I. Kim, H. Hosoda, and S. Miyazaki, "Mechanical properties and shape memory behavior of Ti–Nb alloys," *Mater. Trans.,* **45**, No. 7, 2443–2448 (2004).
8. L. C. Zhang, T. Zhou, S. P. Alpay, and M. Aindow, "Origin of pseudoelastic behavior in Ti–Mo-based alloys," *Appl. Phys. Lett.,* **87**, No. 24, 241909 (2005).
9. L. H. de Almeida, I. N. Bastos, I. D. Santos, A. J. B. Dutra, C. A. Nunes, and S. B. Gabriel, "Corrosion resistance of aged Ti–Mo–Nb alloys for biomedical applications," *J. Alloys Comp.,* **615**, 666–669 (2014).
10. C. Zhang, H. Tian, C. Hao, J. Zhao, Q. Wang, E. Liu, and C. Dong, "First-principles calculations of elastic moduli of Ti–Mo–Nb alloys using a cluster-plus-glue-atom model for stable solid solutions," *J. Mater. Sci.,* **48**, No. 8, 3138–3146 (2013).
11. Y. Al-Zain, Y. Sato, H. Y. Kim, H. Hosoda, T. H. Nam, and S. Miyazaki, "Room temperature aging behavior of Ti–Nb–Mo-based superelastic alloys," *Acta Mater.,* **60**, No. 5, 2437–2447 (2012).
12. D. C. Zhang, Y. F. Mao, Y. L. Li, J. J. Li, M. Yuan, and J. G. Lin, "Effect of ternary alloying elements on microstructure and superelasticity of Ti–Nb alloys," *Mater. Sci. Eng., A,* **559**, 706–710 (2013).
13. V. N. Eremenko and L. A. Tret'yachenko, *Ternary Systems of Titanium with Transition Metals from Groups IV–VI* [in Russian], Naukova Dumka, Kiev (1987).
14. V. Cheverikin, G. Ghosh, A. Makudera, and J.-C. Tedenac, "Mo–Nb–Ti ternary phase diagram evaluation," in: G. Effenberg (editor), Materials Science International, Stuttgart (2015), Document ID 10.21856.1.1; http://www.msi-eureka.com/preview-html/10.21856.1.1/Mo-Nb-Ti_Ternary_ Phase_Diagram_Evaluation/.
15. N. N. Sobolev, V. I. Levanov, O. P. Elyutin, and V. S. Mikheev, "Construction of the diagram of melting for the Ti–V–Nb–Mo system by the simplex lattice method," *Izv. Akad. Nauk SSSR. Metally,* No. 2, 217–221 (1974).
16. I. I. Kornilov and R. S. Polyakova, "Diagrams of state for the ternary titanium–niobium–molybdenum system," *Zh. Neorg. Khim.,* **3**, No. 4, 879–888 (1958).
17. O. M. Myslyvchenko, A. A. Bondar, V. F. Gorban, Yu. F. Lugovskyi, V. B. Sobolev, and I. B. Tikhonova, "Structure and physicomechanical properties of cast titanium alloys of the Ti–Nb–Mo system," *Fiz.-Khim. Mekh. Mater.,* **56**, No. 2, 81–87 (2020); ***English translation:*** *Mater. Sci.,* **56**, No. 2, 224–231 (2020).
18. Yu. A. Kocherzhinskii, E. A. Shishkin, and V. I. Vasilenko, DTA apparatus with a thermocouple sensor of up to 2200°C," in: N. V. Ageev and O. S. Ivanov (editors), *Diagrams of State of Metallic Systems* [in Russian], Nauka, Moscow (1971), pp. 245–249.
19. V. A. Kuz'menko, *Sonic and Ultrasonic Oscillations in the Dynamic Testing of Materials* [in Russian], Izd. Akad. Nauk Ukr. SSR, Kiev (1963).
20. S. A. Firstov, V. F. Gorban, and É. P. Pechkovskii, "Determination of the ultimate values of hardness, elastic strains, and corresponding stresses for materials by the method of automatic indentation," *Materialovedenie,* No. 8, 15–21 (2008).
21. H. S. Kim, W. Y. Kim, and S. H. Lim, "Microstructure and elastic modulus of Ti–Nb–Si ternary alloys for biomedical applications," *Scr. Mater.,* **54**, No. 5, 887–891 (2006).
22. R. Davis, H. M. Flower, and D. R. F. West, "Martensitic transformations in Ti–Mo alloys," *J. Mater. Sci.,* **14**, No. 3, 712–722 (1979).